Applied Surface Science 457 (2018) 1202–1207

Contents lists available at ScienceDirect

Applied Surface Science

journal homepage: www.elsevier.com/locate/apsusc

Full Length Article

Fabrication of high integrated microlens arrays on a glass substrate for 3D micro-optical systems

Yang Wei[a,b], Qing Yang[a,b,*], Hao Bian[a,c], Feng Chen[a,c,*], Minjing Li[a,b], Yanzhu Dai[c], Xun Hou[c]

[a] State Key Laboratory for Manufacturing Systems Engineering, Xi'an Jiaotong University, Xi'an 710049, ShaanXi, People's Republic of China
[b] School of Mechanical Engineering, Xi'an Jiaotong University, Xi'an 710049, ShaanXi, People's Republic of China
[c] Shaanxi Key Laboratory of Photonics Technology for Information, School of Electronics & Information Engineering, Xi'an Jiaotong University, Xi'an 710049, ShaanXi, People's Republic of China

ARTICLE INFO

Keywords:
Microlens array
Femtosecond laser microfabrication
Integrated micro-optics
Imaging patterns

ABSTRACT

Microlens array have been developed as an essential element in integrated micro-optical systems. However, rapidly fabrication of high integration, high fill factor and multi-layer microlens arrays on a hard material is still a challenge. Here, facilely designed high integrated double-sided concave microlens arrays were proposed. These concave microlens arrays possess nearly 5000 close-packed microlenses on a double sides glass substrate, which were created by femtosecond laser wet etch process. The optical properties of integrated microlens arrays were investigated, which exhibit novel diverse imaging patterns, such as coaxial nested rectangular-shaped, coaxial nested hexagonal-shaped, non-coaxial nested hexagonal-shaped imaging patterns, *etc*. Moreover, diverse imaging patterns can be simply realized by controlling the shape, the size of the microlenses and the arrangement of the microlens arrays on the double-sided glass chips.

1. Introduction

Integrated micro-optical components, such as grating, photonic crystal, microlens array (MLA), have been emerged as crucial optical elements for the opto- electro- mechanical system [1–7]. Integrated MLA, like high fill factor single layer MLA, which will increase the usage ratio of the light can be considered as a typically 2D integrated optical element. Likewise, multi-layers MLAs which integrate the MLAs on the direction of light propagation will contribute to the 3D integrated micro-optical systems. These integrated MLAs can be potentially applied in laser homogenization [8–12], holographic laser projection [13], optical inspection [14,15], light emission [16,17], *etc* [18,19]. Multi-layers MLA, especially for double-sided MLAs which can be considered as the integrated fly-eye, is one promising optical element for efficient homogeneous illumination [20–22]. Compared with the single layer MLA, the double-sided MLAs can shape the light beam into a suitable optical pattern, enhance the ability of homogenization and increase the uniformity of the light distribution. Moreover, double-sided MLAs are 3D integrated optical elements which show competent for miniaturization optical systems.

Several methods have been proposed to fabricate the MLA, such as atomic layer deposition [23], lithography with expensive masks [24], self-assembly [25], printing [7], reconfigurable micro-templating [26], thermal reflow [27]. Due to the inherent limit, these methods were restricted by certain defects, such as complexity and high cost of fabrication process, poor efficiency and soft materials, which restrict practical applications. For instance, Li et al. presented a vapor-induced dewetting method for fabricating MLAs on polymeric surfaces [28]. This method concentrates on the polymer materials which is impractical in high temperature and complex applications. In particular, this method cannot realize high-fill factor and coaxial microlenses on double sides of substrate. Huang et al. fabricated a double-sided MLA by a glass molding technique. Nevertheless, this method is restricted to poor efficiency and lack of controllability [29]. As a consequence, rapidly fabrication of high fill factor, shape and size controllable microlenses and high coaxial double-sided 3D integrated MLAs are still a challenge.

Femtosecond laser micromachining have been demonstrated processing microstructures in a wide range of materials during our previous work [30–33]. Here, we introduce a novel structure of integrated double-sided concave microlens arrays (DSC-MLAs) on a glass chip which will contribute to the 3D micro-optical systems. The fabrication method involved a femtosecond laser wet etch (FLWE) process, which shows high efficiency for the whole fabrication process can be finished

* Corresponding authors at: State Key Laboratory for Manufacturing Systems Engineering, Xi'an Jiaotong University, Xi'an 710049, ShaanXi, People's Republic of China.
E-mail addresses: chenfeng@mail.xjtu.edu.cn (Q. Yang), yangqing@mail.xjtu.edu.cn (F. Chen).

https://doi.org/10.1016/j.apsusc.2018.06.267
Received 26 March 2018; Received in revised form 13 June 2018; Accepted 27 June 2018
Available online 28 June 2018
0169-4332/

within 2 h. The fabricated DSC-MLAs possess nearly 5000 highly coaxial close-packed microlenses on each side of substrate. The arrangement, size and shape of microlenses were varied on two sides of glass chips to realize the diverse DSC-MLAs. Moreover, the morphology and the optical properties, such as imaging, optical focusing and optical homogenization of the DSC-MLAs were investigated.

2. Experimental

In this work, the FLWE method was utilized to achieve the DSC-MLAs. Firstly, a femtosecond laser beam (Pulse duration: 50 fs, central wavelength: 800 nm, reputation rate: 1 kHz) was focused by an objective lens (50×, NA = 0.6). The focused laser was subsequently irradiated on one side of the commercial K9 glass chips (thickness: 0.9 mm). In order to balance the efficiency and the uniformity of the microlenses, the exposure time was kept for 500 ms of each exposure spots [34]. Then turned over the sample, repeated the process on the opposite side of the glass chip. The coaxial exposure spots arrays on the double-sided were controlled by an *x-y-z* translation stage and an extra rotary stage with computer program. Secondly, the sample was treated by the chemical wet etch under low power ultrasonic bathing (40 kHz). The chemical solution contained 10% concentration of the hydrofluoric acid. The concave microlens structure would be subsequently formed by the selective chemical etch process. In addition, different sizes of the microlenses were obtained by controlling the laser power, exposure time and etch time. After chemical treating for several-tens of minutes, the DSC-MLA which contains 5000 close-packed microlenses on each side would be finally created. Diverse double-sided MLAs which contained special shaped microlenses, like coaxial rectangular-shaped and hexagonal-shaped would be obtained by a facile arrangement MLA on each side of the glass chips.

3. Results and discussion

The superiority of the beam shaping performance demonstrated here relies on the diverse imaging patterns they can produce. Firstly, the coaxial rectangular-shaped and the coaxial hexagonal-shaped DSC-MLAs were fabricated. Insets of the Fig. 1(b, c) show the arrangement of exposure spots on each side of the glass chip. Herein, the solid sphere and the dotted sphere respectively represent the top side and the bottom side exposure spots, which are coinciding with the other side. In details, the distance of the adjacent laser-pulse-induced craters is set for 60 μm. The femtosecond laser beam energy of each exposure spot is kept for 4 μJ, the diameter of the spots is about 1.4 μm. So that the laser fluence is computed for about 2.6×10^2 J/cm^2. The imaging properties of the coaxial DSC-MLAs were investigated by using a traditional optical imaging system (Fig. 1(a)). It contains a charge-coupled device (CCD), a commercial optical microscope (Nikon, 10×, NA = 0.3; 20×, NA = 0.4) and a white light source. As shown in Fig. 1(b, c), the observation images show that each concave microlens on top side performed as an "eye", which can be used to observe the MLAs on bottom side. As the result, we can respectively get the periodic arrangement of the rectangular-shaped and hexagonal-shaped group patterns, which respectively contain the similar periodic rectangular and hexagonal MLA in each group. Each group looks like the miniaturized compound eye in nature, which can be considered as a compound patterns. Then a transparent letter "A" with black backdrop film was placed between the sample and the light source. The imaging results Fig. 1(d, e) show that the clear rectangular-shaped and hexagonal-shaped arrangement of letters "A" are orderly arranged in each group, which are respectively marked by the red wireframe.

Particularly, the fabricated coaxial DSC-MLAs were respectively investigated by the scanning electron microscope (Fig. 2(a, b)). Insets are magnified images which show the highly consistent of each microlenses. The cone craters with lots of periodic nano stripes would be produced by laser irradiation, these structures would be rapidly etched by chemical solution. Then the rectangular-shaped and hexagonal-shaped microlenses would be formed until the adjacent concave structures "squeezed" each other by a chemical etch process. The roughness of an area of 5 μm × 5 μm on the bottom surface of the microlens structures was measured, which show the average roughness was 19.32 nm. The 3D morphologies of the microlenses were investigated by the laser scanning confocal microscope (Fig. 2(c, d)). The cross-sectional profiles are respectively showed in Fig. 2(e, f), the red dots represent the measured data, and the black curve lines represent fitting data of the ideally parabolic which show the superb contact ratio with the measured data. Respectively, the measured diameters and the sag heights standard deviations of the microlens are 0.34 μm and

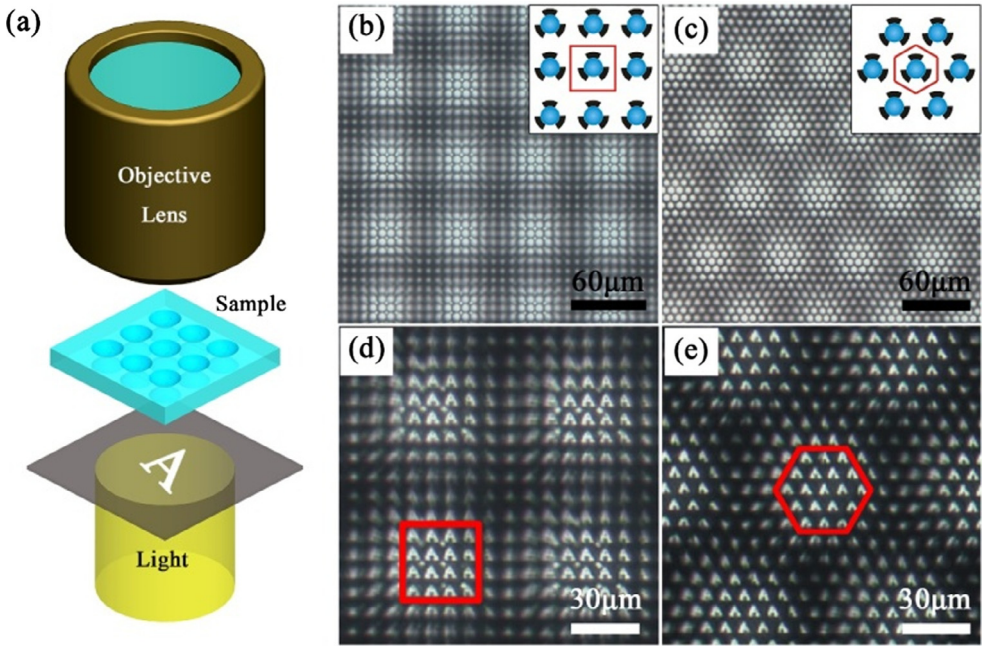

Fig. 1. (a) Schematic illustration of the microscopic imaging system. (b, c) The bottom side of the MLA observed by the top side of the MLA (insets respectively represent the arrangement of the rectangular-shaped and hexagonal-shaped MLAs on each side). (d, e) Imaging properties of the letter "A".

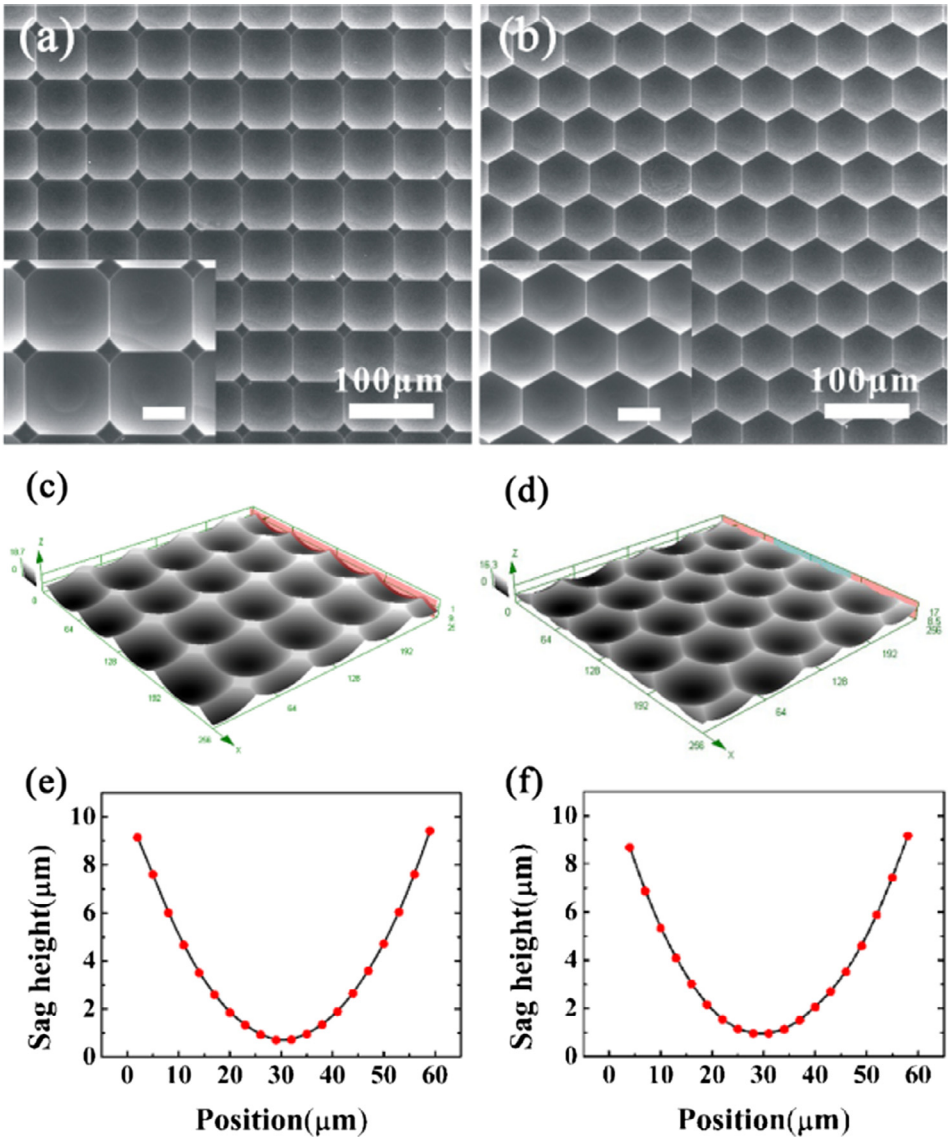

Fig. 2. (a, b) SEM images of the rectangular-shaped and hexagonal-shaped MLAs, insets are the magnified images, scale bar: 30 μm. (c, d) 3D morphologies of each shape MLA. (e, f) Fitting parabolic of the cross-sectional profile.

0.05 μm. The focal length of the microlens can be calculated according to formula $f = (R^2 + h^2)/2h(n\text{-}1)$, where R and h respectively represent the radius and the sag height of the microlens. Herein, R is 30 μm which is the half distance of the exposure spots we designed previously, the h is 8.962 μm which investigated by the laser scanning confocal microscope, and n is the glass reflective index which is 1.516. Therefore, we get the computing results f is 105.99 μm.

In addition, the optical imaging properties of the coaxial rectangular-rectangular double-sided MLAs, the coaxial hexagonal-hexagonal double-sided MLAs, the rectangular-hexagonal double-sided MLAs and non-coaxial hexagonal-hexagonal double-sided MLAs were respectively investigated. Fig. 3(a, b) respectively show the light-spot imaging patterns of the coaxial rectangular-rectangular and hexagonal-hexagonal double-sided MLAs. While the beam passes through the MLAs, the beam will firstly divide into lots of beamlets by the bottom side MLA. Owing to the refraction of the bottom side concave MLA, the beamlets diffuse from the bottom side MLA to the top side MLA. Due to the different refractive index between glass and air, each microlens on the top side collect beamlets and focus them at last. As the result, it is obvious that the rectangular arrangement and the hexagonal arrangement of the light spots are respectively orderly arranged in each group. These groups are also respectively arranged as the rectangle and the hexagon. These novel images can be called as the coaxial nested rectangular-shaped and the coaxial nested hexagonal-shaped imaging patterns. The imaging patterns in Fig. 3(c) coming from the periodic rectangular-shaped and hexagonal-shaped MLAs, which are respectively arranged on the opposite sides of the glass chips. The hexagonal-shaped MLA is on the bottom side and the rectangular-shaped MLA is on the top side. According to the imaging patterns, the groups are rectangular arrangement, in which contain the hexagonal arrangement of the light-spots. Fig. 3(d) shows the imaging patterns of the non-coaxial hexagonal-hexagonal double-sided MLAs. During the irradiation process, the exposure spots on the top side are not coaxial to the bottom side. Comparing with the Fig. 3(b), the boundary between each group of the Fig. 3(d) is larger than the Fig. 3(b). Especially, the light spots array in each group is not coaxial to the group array. According to these diverse light-spot imaging patterns, the bottom side of the MLA determines the arrangement of the light-spot in each focus group, and the top side of the MLA determines the arrangement of the focus group. With the combination of the diverse shapes of the microlenses, the DSC-MLAs can produce diverse imaging patterns.

Moreover, the different diameters of rectangular-shaped MLAs on

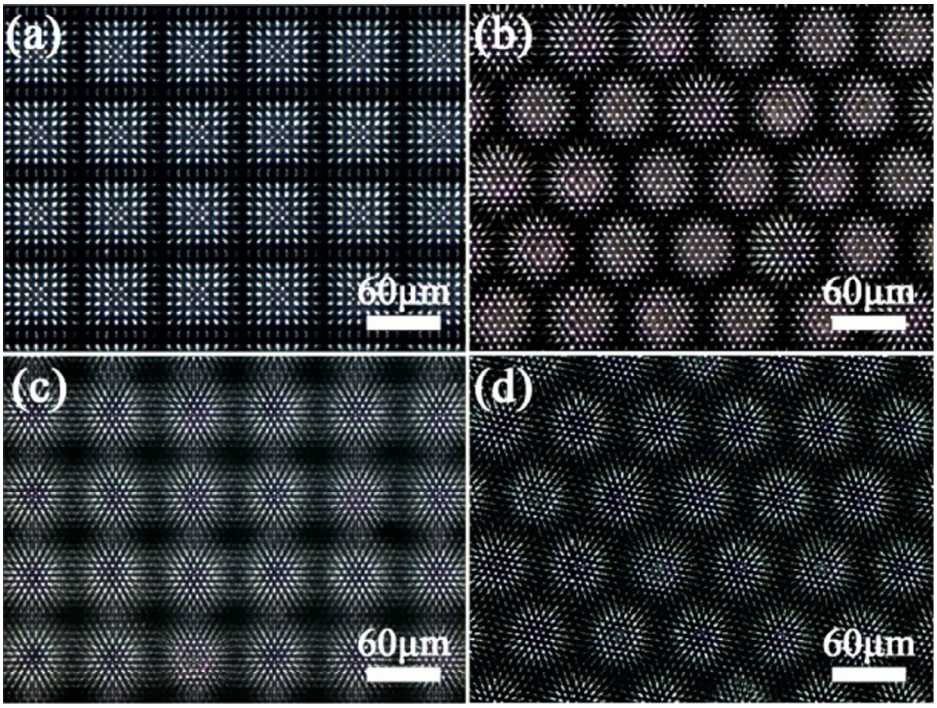

Fig. 3. The imaging patterns of (a) the coaxial rectangular-rectangular double-sided MLAs, (b) the hexagonal-hexagonal double-sided MLAs, (c) the rectangular-hexagonal double-sided MLAs and (d) the non-coaxial hexagonal-hexagonal double-sided MLAs.

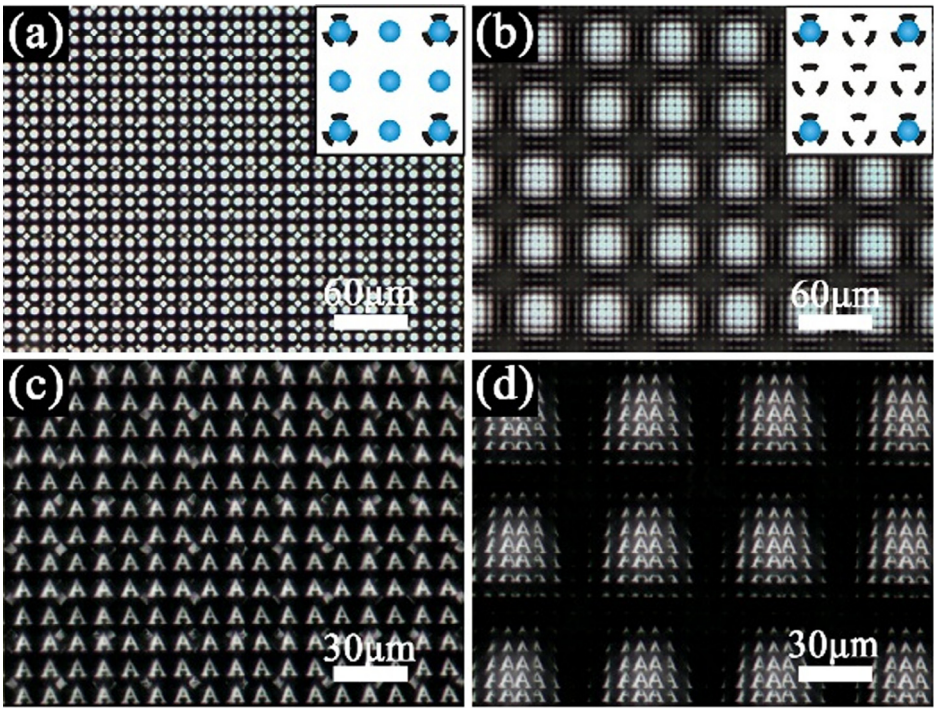

Fig. 4. (a, b) The DSC-MLA with the top side of the microlens for the diameter of 50 μm and 100 μm (insets are the arrangement of the different diameter MLAs on each side). (c, d) Imaging properties of the microlenses for different diameters.

the opposite sides glass chips were fabricated. Fig. 4(a, b) respectively represent the imaging patterns of double-sided MLAs with different diameters. Inset of the Fig. 4(a) represents the arrangement of exposure spots, for which the diameter of microlens on top side is 50 μm (energy of irradiation laser: 3 μJ), and the diameter of microlens on bottom side is 100 μm (energy of irradiation laser: 6 μJ). Inset of the Fig. 4(b) shows arrangement of exposure spots, for which the the diameter of microlenses on top side are 100 μm and on bottom side are 50 μm. The solid sphere and the dotted sphere respectively represent the top side and the bottom side of the exposure spots. The result in Fig. 4(a) demonstrates the uniform distribution of the imaging spots that we can't see clear boundary between each group as presented in Figs. 1 and 3. However, the Fig. 4(b) shows the clear boundary between each group. The imaging properties of the letter "A" are respectively shown in Fig. 4(c, d). The results show that while the diameters of microlens on top side is 50 μm, it would produce the uniform letters "A". However, it would

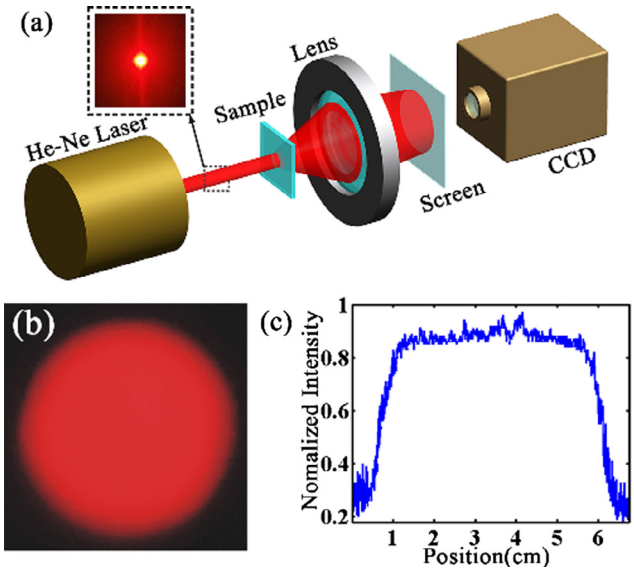

Fig. 5. (a) The schematic illustration of the optical distribution analyzing system. (b) Illumination distribution of the output beam. (c) Normalized intensity distribution curves at the central line of the Fig. 5(b).

produce the group letters "A" with clear boundary when the diameter of the microlens on top side is 100 μm. The microlens array on the bottom side determines the arrangement of the letters "A" in each group and the microlens array on the top side determines the arrangement of the groups. By comparing the microlenses on the bottom side for the different diameters at 100 μm and 50 μm, the larger diameters of microlenses would lead to a larger distance between each letter "A". The width of the boundary between each group extremely closes to the distance between each letter "A". Hence, we cannot distinguish the group and cannot see any boundary in Fig. 4(c). However, in Fig. 4(d), the width of the boundary between each group is much larger than the distance between letters "A", so we can see clear boundary between each group. This characteristic can be used to produce the uniform imaging pattern.

To investigate the characteristics of the optical homogenization of the fabricated coaxial rectangular-shaped DSC-MLA, a simple optical system was utilized to analyze the intensity distribution of the laser beam. The schematic illustration of the optical system is shown in Fig. 5(a). The light source is a He-Ne laser with wavelength of 632 nm (the central width of the beam: 0.5 mm) which is shown in inset of the Fig. 5(a). The laser passed through the sample and then focused by a commercial convex lens (Nikon, 20×, NA = 0.4). After that, the beam was projected on a screen which showed a circular uniform beam. The circular uniform beam was subsequently observed by a CCD which shown in Fig. 5(b). Finally, the normalized intensity distribution at the central horizontal line of the illumination distribution was analyzed and plotted as curves line in Fig. 5(c). The distribution of the illumination with full-width-at-half-maximum (FWHM) is measured for 4.9 cm, and the intensity distribution curve were measured as a flat top. The incident He-Ne laser is typically a Gaussian distribution. When the beam passed through the sample, it would be split into thousands of small beamlets. The highly-centralized Gaussian beam would transform into uniform distributed beams, which demonstrate that the sample owns favorable homogenization.

4. Conclusion

In summary, we reported an integrated double-sided concave MLAs which can produce diverse imaging patterns. The FLWE method was utilized to efficiently fabricate this novel double-sided MLAs, it contains the integrated and high precision coaxial microlenses on double sides of a glass chip. The fabricated double-sided MLAs can produce novel diverse imaging patterns, like coaxial nested rectangular-shaped, coaxial nested hexagonal-shaped, non-coaxial nested hexagonal-shaped and combination of nested rectangular-shaped with hexagonal-shaped imaging patterns, *etc*. We presented that these imaging patterns can be simply realized by varying the size, the shape of the microlens and the arrangement of the microlenses on each side of the glass chips. Moreover, these integrated double-sided MLAs also showed the excellent optical focusing performance and the optical homogenization. We believe that these integrated double-sided MLAs may contribute to the manufacturing of integrated micro-optical systems and have potential applications for laser beam shaping, light emission, photolithography, projection and micro-optical processing.

Acknowledgments

This work is supported by the National Science Foundation of China under the Grant Nos. 51335008 and 61475124, the NSAF Grant No. U1630111, the Special-funded programme on national key scientific instruments and equipment development of China under the Grant No. 2012YQ12004706, the Collaborative Innovation Center of Suzhou Nano Science and Technology and the International Joint Research Center for Micro/Nano Manufacturing and Measurement Technologies. The SEM work was done at International Center for Dielectric Research (ICDR), Xi'an Jiaotong University.

References

[1] S.S. Lee, L.Y. Lin, M.C. Wu, Surface-micromachined free-space micro-optical systems containing three-dimensional microgratings, Appl. Phys. Lett. 67 (1995) 2135–2137.
[2] V. Bhatia, A.M. Vengsarkar, Optical fiber long-period grating sensors, Opt. Lett. 21 (1996) 692–694.
[3] S. Behera, J. Joseph, Single-step optical realization of bio-inspired dual-periodic motheye and gradient-index-array photonic structures, Opt. Lett. 41 (2016) 3579–3582.
[4] M. Campbell, D.N. Sharp, M.T. Harrison, R.G. Denning, A.J. Turberfield, Fabrication of photonic crystals for the visible spectrum by holographic lithography, Nature 404 (2000) 53–56.
[5] N.H. Vu, T.T. Pham, S. Shin, Modified optical fiber daylighting system with sunlight transportation in free space, Opt. Express 24 (2016) A1528–A1545.
[6] Y. Luo, L. Wang, Y. Ding, H. Wei, X. Hao, D. Wang, Y. Dai, J. Shi, Direct fabrication of microlens arrays with high numerical aperture by ink-jetting on nanotextured surface, Appl. Surf. Sci. 279 (2013) 36–40.
[7] X. Zhu, L. Zhu, H. Chen, L. Yang, W. Zhang, Micro-ball lens structure fabrication based on drop on demand printing the liquid mold, Appl. Surf. Sci. 361 (2016) 80–89.
[8] F. Wippermann, U.D. Zeitner, P. Dannberg, A. Brauer, S. Sinzinger, Beam homogenizers based on chirped microlens arrays, Opt. Express 15 (2007) 6218–6231.
[9] P.H. Yao, C.H. Chen, C.H. Chen, Low speckle laser illuminated projection system with a vibrating diffractive beam shaper, Opt. Express 20 (2012) 16552–16566.
[10] C. Kopp, L. Ravel, P. Meyrueis, Efficient beamshaper homogenizer design combining diffractive optical elements, microlens array and random phase plate, J. Opt. A: Pure Appl. Opt. 1 (1999) 398–403.
[11] F. Nikolajeff, S. Hård, B. Curtis, Diffractive microlenses replicated in fused silica for excimer laser-beam homogenizing, Appl. Opt. 36 (1997) 8481–8489.
[12] S. Pfadler, F. Beyrau, M. Loffler, A. Leipertz, Application of a beam homogenizer to planar laser diagnostics, Opt. Express 14 (2006) 10171–10180.
[13] J.W. Pan, C.M. Wang, H.C. Lan, W.S. Sun, J.Y. Chang, Homogenized LED-illumination using microlens arrays for a pocket-sized projector, Opt. Express 15 (2007) 10483–10491.
[14] A.I. Kuznetsov, A.B. Evlyukhin, M.R. Goncalves, C. Reinhardt, A. Koroleva, M.L. Arnedillo, R. Kiyan, O. Marti, B.N. Chichkov, Laser fabrication of large-scale nanoparticle arrays for sensing applications, ACS Nano 5 (2011) 4843–4849.
[15] J. Li, W. Liu, T. Li, I. Rozen, J. Zhao, B. Bahari, B. Kante, J. Wang, Swimming microrobot optical nanoscopy, Nano Lett. 16 (2016) 6604–6609.
[16] S.I. Chang, J.B. Yoon, H. Kim, J.J. Kim, B.K. Lee, D.H. Shin, Microlens array diffuser for a light-emitting diode backlight system, Opt. Lett. 31 (2006) 3016–3018.
[17] P. Melpignano, V. Biondo, S. Sinesi, M.T. Gale, S. Westenhöfer, M. Murgia, S. Caria, R. Zamboni, Efficient light extraction and beam shaping from flexible, optically integrated organic light-emitting diodes, Appl. Phys. Lett. 88 (2006) 153514.
[18] L. Dong, A.K. Agarwal, D.J. Beebe, H. Jiang, Adaptive liquid microlenses activated by stimuli-responsive hydrogels, Nature 442 (2006) 551–554.
[19] S. Sumriddetchkajorn, Micromechanics-based digitally controlled tunable optical beam shaper, Opt. Lett. 28 (2003) 737–739.
[20] T. Gissibl, S. Thiele, A. Herkommer, H. Giessen, Two-photon direct laser writing of ultracompact multi-lens objectives, Nature Photon. 10 (2016) 554–560.

[21] A. Arbabi, E. Arbabi, S.M. Kamali, Y. Horie, S. Han, A. Faraon, Miniature optical planar camera based on a wide-angle metasurface doublet corrected for monochromatic aberrations, Nat. Commun. 7 (2016) 13682.
[22] J. Gong, B. Xu, X. Tao, Breath figure micromolding approach for regulating the microstructures of polymeric films for triboelectric nanogenerators, ACS Appl. Mat. Interfaces 9 (2017) 4988–4997.
[23] M. Khorasaninejad, W.T. Chen, R.C. Devlin, J. Oh, A.Y. Zhu, F. Capasso, Metalenses at visible wavelengths: Diffraction-limited focusing and subwavelength resolution imaging, Science 352 (2016) 1190–1194.
[24] M. Khorasaninejad, Z. Shi, A.Y. Zhu, W.T. Chen, V. Sanjeev, A. Zaidi, F. Capasso, Achromatic metalens over 60 nm bandwidth in the visible and metalens with reverse chromatic dispersion, Nano Lett. 17 (2017) 1819–1824.
[25] J.Y. Lee, B.H. Hong, W.Y. Kim, S.K. Min, Y. Kim, M.V. Jouravlev, R. Bose, K.S. Kim, I.-C. Hwang, L.J. Kaufman, C.W. Wong, P. Kim, K.S. Kim, Near-field focusing and magnification through self-assembled nanoscale spherical lenses, Nature 460 (2009) 498–501.
[26] K.H. Jeong, J. Kim, L.P. Lee, Biologically inspired artificial compound eyes, Science 312 (2006) 557–561.
[27] W. Choi, R. Shin, J. Lim, S. Kang, Design methodology for a confocal imaging system using an objective microlens array with an increased working distance, Sci. Rep. 6 (2016) 33278.
[28] X. Bi, W. Li, Fabrication of flexible microlens arrays through vapor-induced dewetting on selectively plasma-treated surfaces, J. Mater. Chem. C 3 (2015) 5825–5834.
[29] C.Y. Huang, W.T. Hsiao, K.C. Huang, K.S. Chang, H.Y. Chou, C.P. Chou, Fabrication of a double-sided micro-lens array by a glass molding technique, J. Micromech. Microeng. 21 (2011) 085020.
[30] J.L. Yong, Y. Fang, F. Chen, J.L. Huo, Q. Yang, H. Bian, G.Q. Du, X. Hou, Femtosecond laser ablated durable superhydrophobic PTFE films with micro-through-holes for oil/water separation: Separating oil from water and corrosive solutions, Appl. Surf. Sci. 389 (2016) 1148–1155.
[31] J.L. Yong, F. Chen, Q. Yang, Y. Fang, J. Huo, J. Zhang, X. Hou, Nepenthes inspired design of self-repairing omniphobic slippery liquid infused porous surface (SLIPS) by femtosecond laser direct writing, Adv. Mater. Interfaces 4 (2017) 1700552.
[32] F. Chen, Z. Deng, Q. Yang, H. Bian, G. Du, J. Si, X. Hou, Rapid fabrication of a large-area close-packed quasi-periodic microlens array on BK7 glass, Opt. Lett. 39 (2014) 606–609.
[33] H. Bian, Y. Wei, Q. Yang, F. Chen, F. Zhang, G. Du, J. Yong, X. Hou, Direct fabrication of compound-eye microlens array on curved surfaces by a facile femtosecond laser enhanced wet etching process, Appl. Phys. Lett. 109 (2016) 221109.
[34] Z. Deng, F. Chen, Q. Yang, H. Liu, H. Bian, G. Du, Y. Hu, J. Si, X. Meng, X. Hou, A facile method to fabricate close-packed concave microlens array on cylindrical glass, J. Micromech. Microeng. 22 (2012) 115026.